

Griffiths-like phase and magnetic correlations at high fields in Gd₅Ge₄Nicolás Pérez,¹ Fèlix Casanova,² Fernando Bartolomé,³ Luis M. García,³ Amílcar Labarta,¹ and Xavier Batlle^{1,*}¹*Departament de Física Fonamental and Institut de Nanociència i Nanotecnologia IN²UB, Universitat de Barcelona, Martí i Franquès 1, 08028 Barcelona, Catalonia, Spain*²*CIC nanoGUNE, 20018 Donostia-San Sebastian, and IKERBASQUE, Basque Foundation for Science, 48011 Bilbao, Basque Country, Spain*³*Instituto de Ciencia de Materiales de Aragón, CSIC-Universidad de Zaragoza, Departamento de Física de la Materia Condensada, Pedro Cerbuna 12, 50009 Zaragoza, Spain*

(Received 21 July 2010; revised manuscript received 18 March 2011; published 17 May 2011)

Magnetic correlations appearing in polycrystalline Gd₅Ge₄ are studied. On the one hand, ac susceptibility measurements as functions of temperature at several dc fields and frequencies show the existence of ferromagnetic (FM) and antiferromagnetic (AFM) correlations in the paramagnetic (PM) region, where a Griffiths-like phase appears below ~ 225 K. The value for the effective magnetic moment within the Griffiths-like phase is $10.1 \mu_B$. FM correlations also extended all the way into the AFM phase below ~ 127 K. The onset of the Griffiths-like phase is associated with an effective critical slowing down. On the other hand, high field magnetization measurements reveal the presence of FM and AFM correlations in the three magnetic phases (PM, FM, and AFM), giving rise to a variety of mixed magnetic states. In particular, at high fields the magnetostructural transition takes place in several stages that extend along a wide temperature range. A three-dimensional (T, H, M) phase diagram is proposed, including the new experimental findings.

DOI: [10.1103/PhysRevB.83.184411](https://doi.org/10.1103/PhysRevB.83.184411)

PACS number(s): 75.30.Sg, 75.30.Kz

I. INTRODUCTION

The coexistence of magnetic interactions of opposite nature within a material leads to complex magnetic behavior that may give rise to a rich variety of physical phenomena. The intermetallic compound Gd₅Ge₄ has recently received much attention^{1–18} due to the unusual magnetic behavior originating from the competition of ferromagnetic (FM) and antiferromagnetic (AFM) interactions present in its layered crystal structure.¹ One of the most interesting features is the field-induced metamagnetic transition between AFM and FM states, which is coupled to a structural change² that gives the first-order nature of the transition. This magnetostructural transition yields a large variety of magnetoresponsive phenomena, such as giant magnetocaloric effect,^{2–4,19} giant magnetoresistance,⁵ large magnetostriction,^{6,20} acoustic emission²¹ or avalanche processes.^{22,23} Although the equilibrium thermodynamic ground state at low temperatures is FM,⁸ as in Si-doped compounds,⁹ the AFM state is maintained when cooling down in the absence of an applied magnetic field, due to a kinetic arrest⁸ that can be overcome by the application of magnetic field. This explains the switch from reversible to irreversible nature of the transition at low temperatures.^{4,10,11} The transition can be induced not only by magnetic field or temperature, but also by Si substitution¹² or pressure.¹³ In addition, Gd₅Ge₄ shows the presence of a Griffiths-like (GL) phase in the paramagnetic (PM) region,¹⁴ short-range FM correlations in the AFM and PM regions at high fields,⁹ or a spin-flop transition in the AFM phase.¹⁵

The competing FM and AFM interactions in Gd₅Ge₄ arise from its naturally layered crystal structure.² In the AFM state, the magnetic moments of Gd within each layer are FM coupled, whereas the alignment between layers is AFM, as suggested by Levin *et al.*¹⁵ and confirmed by x-ray magnetic resonant scattering experiments.¹⁶ During the structural transition, shear of the layers enhances Ge–Ge bonds between adjacent layers,² favoring the FM alignment and thus a FM state. The

high sensitivity of the Ge–Ge bonds to magnetic field, thermal fluctuations, and structural defects (interstitial impurities, residual phases, vacancies, grain boundaries in the case of polycrystals, etc.), results in a degree of disorder in the layered structure that causes magnetic frustration, leading to a nonhomogeneity of the magnetic state throughout the material. In fact, it has been previously observed by Hall probe imaging how the magnetostructural transition between the AFM and FM phases occurs via nucleation and growth of irregular domains of one magnetization state inside a “matrix” of the opposite state.¹⁸ Consequently, short-range FM correlations appear along the phase diagram, including a GL phase as a paradigmatic example.^{9,14,17}

In this paper, we study the GL phase by means of ac susceptibility at several low-dc fields and frequencies. We show that the onset of the GL phase takes place in the PM region, yielding an effective critical slowing down associated with competing AFM and FM magnetic correlations. Moreover, the FM correlations extend all the way into the AFM phase. The effective moment in the GL phase and the relation between the GL phase and the crystallographical and chemical disorder are discussed. We also report new competing effects from measurements at high magnetic fields, in the vicinity of the first-order magnetostructural transition, in which AFM correlations are retained in the main FM phase. In addition, short-range FM and AFM clusters are observed in the main phases, usually labeled as PM and AFM. These results unveil the existence of large regions of strongly competing interactions and enable us to propose a three-dimensional (T, H, M) phase diagram.

II. EXPERIMENTAL

Polycrystalline Gd₅Ge₄ samples were synthesized by arc melting in a custom furnace under a high-purity Ar atmosphere. High-purity materials (Ge 99.999 wt % from Aldrich and Gd, sublimed, dendritic, 99.99 wt % REO from Alfa Aesar)

in the desired stoichiometry were used. The samples were placed in a water-cooled copper crucible and melted several times to ensure good homogeneity. The weight losses after arc melting were negligible. After synthesis, the samples were thermally treated inside a quartz tube placed in an electrical resistance furnace for 5 h at 900 °C under a vacuum of 10^{-5} mbars. After annealing, the quartz tube was quickly taken out of the furnace and cooled to room temperature. Electron-beam microprobe analysis confirmed the Gd_5Ge_4 stoichiometry and the absence of secondary phases and magnetic atoms other than Gd. The crystallographic structure of the sample was studied at room temperature by x-ray diffraction. The samples displayed the expected room-temperature orthorhombic structure (Sm_5Ge_4 -type $Pnma$).^{24,25} Ac susceptibility as a function of temperature was measured using a commercial superconducting quantum interference device magnetometer. Both the real (χ') and the imaginary part (χ'') were recorded using an ac magnetic field, h_{ac} , of 4 Oe in amplitude: (a) at several dc magnetic fields, h_{dc} , in the range from 0 to 200 Oe with ac frequency $\nu = 100$ Hz and (b) at several frequencies ν from 0.1 to 1000 Hz with $h_{dc} = 0$. Magnetization measurements at high magnetic fields were carried out in the M6 Bitter magnet at the Laboratoire National des Champs Magnétiques Intenses (formerly the Grenoble High Magnetic Field Laboratory) using a custom extraction magnetometer inside a liquid He flux cryostat. Isothermal magnetization curves, $M(H)$, were recorded, increasing and decreasing the field between 0 and 23 T. Isofield magnetization curves, $M(T)$, were recorded in ramping temperatures within 4.2 and 300 K at a rate of 1 to 2 K/min.

III. RESULTS AND DISCUSSION

A. Ac susceptibility measurements

Figure 1 shows the inverse of χ' as a function of temperature, showing the expected Néel temperature ($T_N \approx 127$ K) where the compound becomes AFM^{3,6,9–11,24} and a large anomaly at $T_G \approx 225$ K. The GL anomaly was previously identified in Gd_5Ge_4 single crystals from dc magnetization measurements.¹⁴ Direct plots of both χ' and χ'' also evidence this anomaly (see Figs. 2 and 3), attributed to the onset of the GL phase.²⁶ The fact that the anomaly appears simultaneously in χ'' and χ' indicates that the onset of the GL phase is accompanied by an energy dissipation process. The fit of the inverse of χ' to a Curie–Weiss law (Fig. 1) provides the effective magnetic moment μ_{eff} and extrapolated Curie temperature θ associated with both the PM and GL phases. The value of the magnetic moment obtained in the GL phase, $\mu_{\text{eff}}^{\text{GL}} = 10.1 \mu_B$, is larger than $\mu_{\text{eff}}^{\text{PM}} = 7.9 \mu_B$ obtained in the PM phase (value that corresponds to the expected for free Gd^{3+} ions), indicating the FM clustering of spins in the former. No further information can be obtained on either the spatial distribution or number of spins involved in the clusters since neutron scattering experiments cannot be carried out in those kind of samples.

The dependence on frequency of χ' in the GL phase is shown in the inset to Fig. 1. A steady decay without any maxima is observed in the frequency range 0.1 to 1 kHz and only an increase of the slope is noticeable at the onset of the

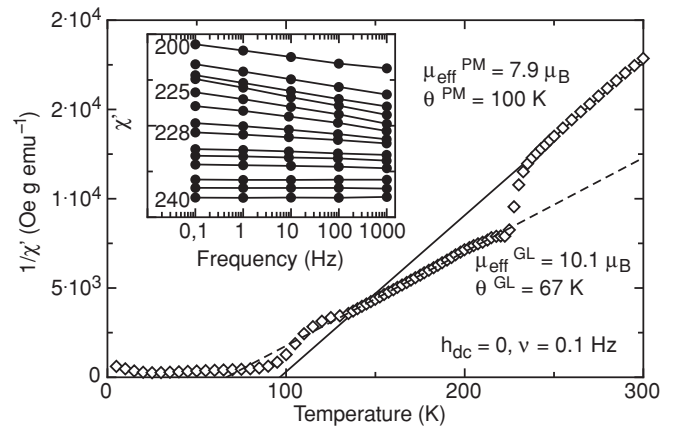


FIG. 1. Inverse of the real part of the ac susceptibility of polycrystalline Gd_5Ge_4 obtained on heating after a zero field cooling process. Curie–Weiss fit is shown for the GL phase region (dashed line) and for the pure PM region (solid line). Inset: Real part of the ac susceptibility as a function of frequency measured at various temperatures (from 200 K, uppermost line, to 240 K, bottom line).

GL anomaly between 228 and 225 K. As the frequency increases, a reduction of the signal in both χ' and χ'' and a slight shift of the anomaly to higher temperatures are shown in Fig. 2(b) and Fig. 3(b). The peak corresponding to the onset of the GL phase shifts from 218 to 220 K when the frequency varies within 0.1 to 1 Hz, this shifting being only in a few tenths of degree in the following three decades. Usually, the dynamics of critical phenomena in correlated and noncorrelated systems is characterized by the shift of the critical temperature per frequency decade.²⁷ This is expressed as $\Delta T_G / [T_G \Delta \log(\omega)]$, where ω is the ac frequency.²⁷ We found that this value is about 0.001 in our samples, which is about two orders of magnitude lower than those found in systems with purely Arrhenius relaxation, such as a noninteracting distribution of fine magnetic particles,²⁷ and lies in the lower end of the typical values found in systems with high magnetic frustration, such as spin glasses.²⁷ This weak frequency dependence is in contrast with that found in the ErCo_2 GL phase,²⁸ where clusters of Co spins coherently rotate, driven by the ac field. In the present case, the correlated spins seem to be strongly pinned, showing weak magnetic response in the frequency range studied. The strong correlations evidenced by the dynamics are in agreement with the increase of the observed $\mu_{\text{eff}}^{\text{GL}}$ with respect to $\mu_{\text{eff}}^{\text{PM}}$. These results suggest that the onset of the GL anomaly is associated with an effective critical slowing down due to the existence of strong magnetic correlations yielding collective excitations rather than due to a pure thermally activated process.

Figure 2(a) shows that the GL anomaly in χ' gradually diminishes with the application of a small dc field, h_{dc} , being barely observable for $h_{dc} = 200$ Oe, in agreement with the extreme sensitivity to the external field shown by the GL phase in other rare earth compounds.^{28–30} The suppression of the anomaly in χ'' by h_{dc} [Fig. 3(a)] without any trace of energy absorption or dissipation at about $h_{dc} \approx 200$ Oe suggests that the mechanism underlying the formation of the GL phase is actually suppressed as the field is increased rather than just hidden by the PM background, as previously

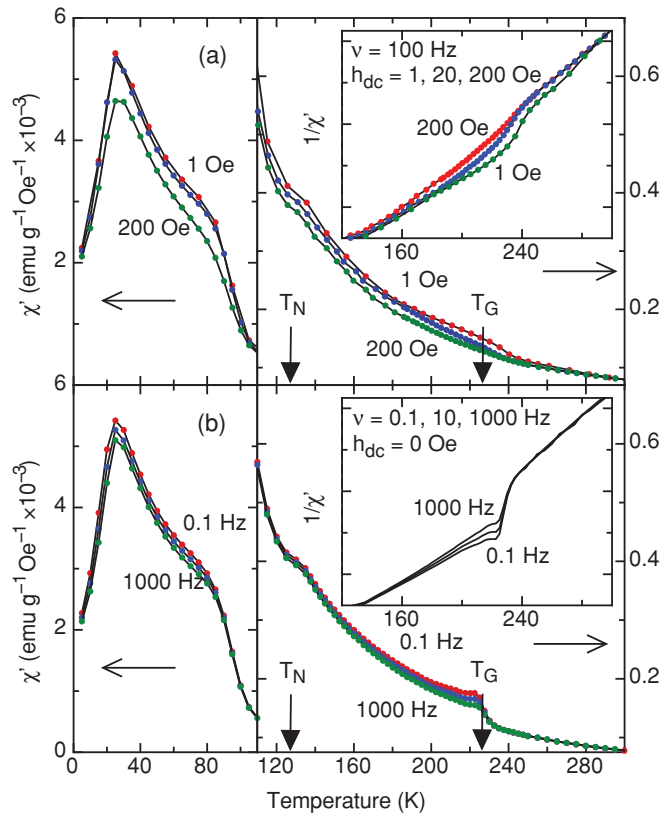


FIG. 2. (Color online) Real part of the ac susceptibility of polycrystalline Gd_5Ge_4 measured at different (a) applied dc fields (1, 20, and 200 Oe) and (b) frequencies (0.1, 1, 10, 100, and 1000 Hz). Note that for $T \geq 110$ K the vertical axis is magnified and values are indicated at the right of the panel. For $T \leq 110$, the vertical axis is given at the left of the panel. Numbers beside the curves indicate the value of the varied parameter. Insets in (a) and (b) show the inverse susceptibility around the GL phase.

suggested for $\text{Tb}_5\text{Si}_2\text{Ge}_2$.³⁰ A comprehensive data set of $(\chi')^{-1}$ in the temperature range T_N – T_G was fitted to the predicted temperature dependence of the susceptibility for a GL phase in f -electron compounds, $\chi^{-1} \propto (T - T_c)^{(1-\lambda)}$,³¹ where T_c denotes the critical temperature and $(1 - \lambda)$ is the effective index with $0 \leq \lambda < 1$. The simultaneous fit of T_c and λ converges to a Curie–Weiss law ($\lambda = 0$). Moreover, Fig. 4 shows the field dependence of the fitted values for T_c , which increasingly approach the Curie–Weiss temperature of the PM region ($\theta^{PM} = 100$ K) as the applied field increases. The reduction of T_c in the GL phase with respect to that of the PM phase indicates the formation of AFM correlations, which are further disfavored by the application of low external fields. Consequently, the system could be composed of ferromagnetically correlated spin clusters, where some degree of AFM correlations may also be present. Taking into account the previous results we suggest that the GL phase originates from the competition of FM and AFM correlations above the Néel temperature, and the application of moderate dc magnetic fields favors the growth of the regions with short-range FM correlations, thus destabilizing the GL phase until it disappears at about 200 Oe. We note that it has recently been shown that local disorder induced by the presence of substituents in

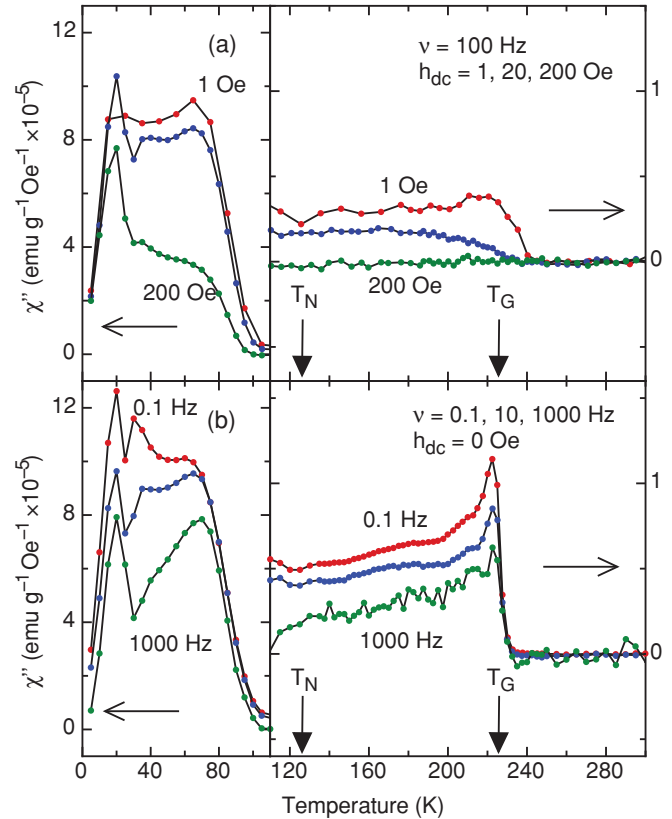


FIG. 3. (Color online) Imaginary part of the ac susceptibility of polycrystalline Gd_5Ge_4 measured at different (a) applied dc fields (1, 20, and 200 Oe) and (b) frequencies (0.1, 1, 10, 100, and 1000 Hz). Note that for $T \geq 110$ K the vertical axis is magnified and values are indicated at the right of the panel. For $T \leq 110$, the vertical axis is given at the left of the panel. Numbers beside the curves indicate the value of the varied parameter.

certain Gd sites of the Gd_5Ge_4 lattice has a strong influence on the magnetic interactions between the Gd ions and leads to severe changes in the magnetic behavior, including an increase of the magnetic moment of the Gd^{3+} ions.³² In this context it is worth noting that samples synthesized with Gd of 99.9 wt % purity, show strong variations in the fitted value of λ yielding $\lambda \approx 0.5$, in contrast with the present case (Gd of 99.99 wt % REO purity), where the best fitted value was always very close to zero. These differences are indicative of the strong sensitivity of the system to the local structural details, which may account for the dispersion of λ values found in literature.^{14,33} Additionally, this suggests that the actual dynamics of the GL phase in Gd_5Ge_4 depends on the local disorder of the system.

In Fig. 2 and 3 it is shown that χ' and χ'' are reduced by the effect of increasing either the dc field or ac frequency. In particular, the steep rise of χ'' just below the Néel temperature, $T_N \approx 127$ K, is severely affected by the dc field. It was previously proposed that below T_N FM clustering of spins occurred down to approximately 75 K.¹⁴ The ac susceptibility measurements presented here are in agreement with those results, evidencing that the FM clustering phenomenon extends down to approximately 20–30 K and displays field and frequency dependencies similar to those of the GL phase.

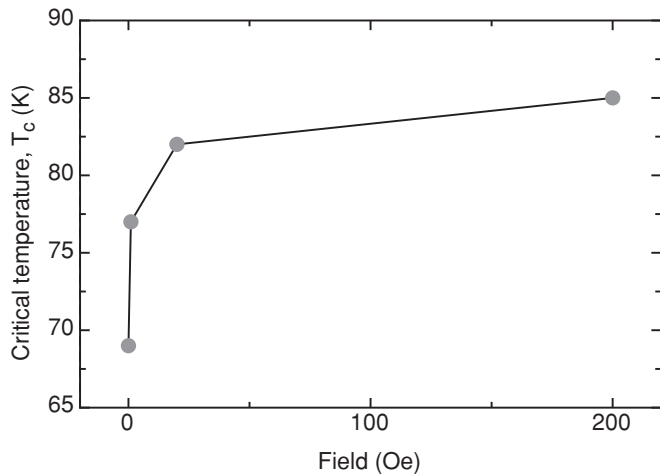


FIG. 4. Variation of the critical temperature with the applied field obtained by fitting χ' within T_N and T_G to the model $\chi'^{-1} \propto (T - T_c)^{(1-\lambda)}$. T_c is given for the applied magnetic fields of 0, 1, 20, and 200 Oe.

B. High field magnetization

Isothermal magnetization curves up to 23 T at several temperatures in Fig. 5 show the shift of the magnetostructural transition to higher critical fields with increasing temperature. At temperatures higher than about 81 K a change in the slope in the curve is clearly evident at about 12 T before the magnetostructural transition occurs, which indicates the break of the long-range AFM ordering and the appearance of FM correlations.⁹ The inset to Fig. 5 shows the irreversible AFM-FM transition at 7 K. Figure 6 shows isofield magnetization as a function of temperature at several magnetic fields, recorded on heating the sample after field cooling from the PM region. We note that the cooling and measuring fields are the same. The zero field cooling curves (not shown) and the field cooling curves measured at fields higher than about 5 T are almost indistinguishable. The anomaly at the Néel temperature disappears at $H \geq 14$ T, and at those fields the magnetization curve tends to follow a linear dependence with temperature in the region usually labeled as PM. Additionally, at $H \geq 10$ T and temperatures immediately below the first-order magnetostructural AFM-FM transition, the system is not completely ferromagnetically ordered: A region of lower magnetization than that of the FM state appears in between the temperature of the magnetostructural transition and the full FM regime (see the encircled area in Fig. 6). This low magnetization region evidences thermal hysteresis when the magnetization is measured cycling the temperature between 4.2 K and room temperature, as the magnetostructural transition does as well (see inset to Fig. 6). The extent of the temperature range of this low magnetization region increases up to ~ 18 T and reduces progressively when the applied field is further increased. Therefore, the estimated amount of sample that is not fully FM is maximum at ~ 18 T, being approximately 10%. Below the magnetostructural AFM-FM transition, the magnetization is not completely saturated down to about 10 K.

The magnetization in the AFM phase increases steadily as the temperature is reduced, in contrast to the expected behavior for a pure AFM phase, due to the favoring of

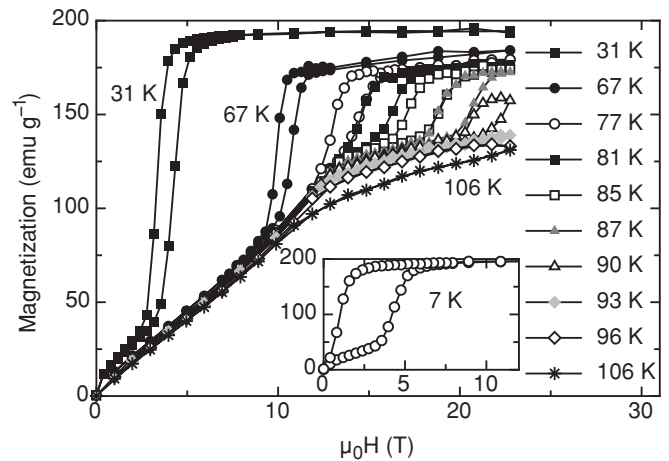


FIG. 5. Isothermal magnetization curves, $M(H)$, of polycrystalline Gd_5Ge_4 at several temperatures, indicated in Kelvin in the legend and next to selected curves, showing the shift of the magnetostructural transition toward higher critical fields with increasing temperature. The curves within 77 and 93 K show a change in the slope associated with clusters of strong FM coupled spins. Inset: $M(H)$ curve for 7 K. Axes have the same units as the ones in main graph.

FM correlations preceding the magnetostructural transition. This is in agreement with a previous work²³ showing that the magnetostructural transition occurs via avalanche processes, displaying training effects when cycling through it. Consequently, the existence of ferromagnetism in the system is not strictly confined to the temperature range below the magnetostructural transition. On the one hand, high magnetic fields reduce the extent of the long-range AFM phase up to its complete vanishing for fields higher than about 12 T and

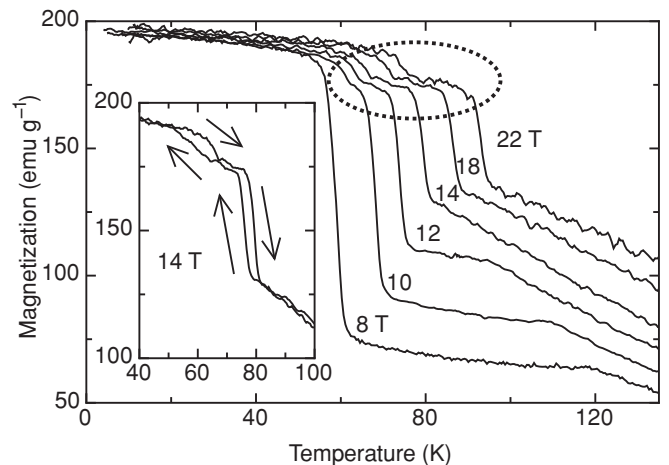


FIG. 6. Isofield magnetization curves, $M(T)$, of polycrystalline Gd_5Ge_4 at several magnetic fields (labeled next to the curve in Tesla) measured on heating after field cooling the sample at those fields. The portion of the curves encircled by the dotted line suggests that the system is not completely FM before the magnetostructural transition. Inset: Example of the hysteresis observed in magnetization on field cooling and field heating the sample at 14 T around the first-order AFM-FM transition.

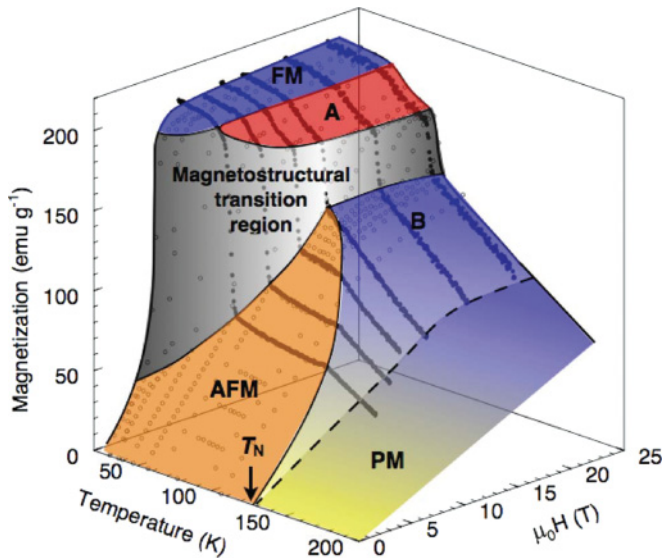


FIG. 7. (Color online) Three dimensional (T, H, M) phase diagram based on the plot of the magnetization as functions of temperature and magnetic field, using high-field measurements. The different magnetic phases are labeled as follows: (PM) paramagnetic phase with ferromagnetic correlations; (AFM) predominantly antiferromagnetic phase with ferromagnetic correlations; (FM) purely ferromagnetic phase; (A) antiferromagnetic short-range correlations in the main ferromagnetic matrix; (B) ferromagnetic and antiferromagnetic short-range correlations in the paramagnetic zone. The dashed line indicates the change of the major character of the magnetic correlations, but it is not a critical boundary.

at the same time enhance FM correlations in the PM phase. On the other hand, the magnetostructural transition does not take place in an abrupt single step, showing at least two clearly identifiable stages.

Figure 7 shows a three-dimensional (T, H, M) phase diagram built up using the $M(T)$ and $M(H)$ curves at high fields that perfectly superimpose along the whole phase diagram. This phase diagram clearly defines the magnetic phase coexistence regions labeled A and B in Fig. 7. When region A is reached following a magnetization isotherm, the system transforms from the AFM state to a partial FM ordering where AFM correlations remain up to 23 T. For magnetization isotherms reaching region B, the system transforms from an AFM state to a nominal PM state where strong FM and AFM correlations coexist, as previously stated.⁹ The magnetic field and the temperature determine the extent of the FM correlations and the size of the PM clusters in a way that, above about the temperatures indicated by the dashed line in Fig. 7,

the PM clusters dominate the behavior of the system, although at moderately high fields FM correlations are noticeable.

IV. SUMMARY AND CONCLUSIONS

Ac susceptibility for Gd_5Ge_4 polycrystals was measured at several applied dc fields and frequencies, evidencing the occurrence of an anomaly at $T_G \approx 225$ K which is associated with the onset of a GL phase. The anomaly showed high sensitivity to the dc field, disappearing gradually and being barely observable at $h_{dc} = 200$ Oe. The effective moment calculated from a Curie–Weiss fit of the inverse of χ' in the GL phase was larger than that of the PM phase, indicating the existence of FM correlations. Besides, the critical temperature increased with the applied field, approaching the value of the Curie–Weiss law found in the PM region. These results indicate the existence of AFM correlations that are disfavored by the application of moderate dc fields. The weak frequency dependence of T_G , similar to that of systems with high degrees of frustration, such as spin glasses, could be associated with an effective critical slowing down. Consequently, on reducing the temperature, T_G determines the onset of a FM clustering regime which originates from magnetic interactions among Gd spins. This regime starts in a nominal PM disorder region, giving rise to a GL phase, and extends into the nominal AFM ordered region.

By combining the $M(T)$ and $M(H)$ curves at high fields, a (T, H, M) magnetic phase diagram was established. In this phase diagram, regions of coexistence of AFM-FM, AFM-PM, and FM-PM phases were clearly identified around the tricritical point at about 81 K and 12 T.

All these magnetic features reveal the existence of regions of strongly competing magnetic interactions where the three main magnetic phases (PM, FM, and AFM) merge in the phase diagram of Gd_5Ge_4 . The combined effect of magnetic field and thermal fluctuations tunes the relative strength of the intrinsic, competing intralayer ferromagnetism and interlayer antiferromagnetism of Gd_5Ge_4 , creating different states of mixed short and long-range magnetic correlations.

ACKNOWLEDGMENTS

The funding of the Spanish MICINN through Project Nos. MAT2009-08667 and MAT2008-1077, Aragonese IMANA E-34, and Catalan DIUE 2009SGR856 is greatly acknowledged. Part of this work was performed at the Laboratoire National des Champs Magnétiques Intenses (LNCMI), under European Community Contract No. RITA-CT-2003-505474. The in-site help of Prof. S. DeBrion and Ms A. Richard in LNCMI is also greatly acknowledged.

*Corresponding author: xavierbatlle@ub.edu

¹D. Paudyal, V. K. Pecharsky, and K. A. Gschneidner Jr., *J. Phys. Condens. Matter* **20**, 235235 (2008).

²V. K. Pecharsky, A. P. Holm, K. A. Gschneidner Jr., and R. Rink, *Phys. Rev. Lett.* **91**, 197204 (2003).

³F. Casanova, A. Labarta, X. Batlle, J. Marcos, L. Mañosa, A. Planes, and S. de Brion, *Phys. Rev. B* **69**, 104416 (2004).

⁴F. Casanova, A. Labarta, and X. Batlle, *Phys. Rev. B* **72**, 172402 (2005).

⁵E. M. Levin, V. K. Pecharsky, K. A. Gschneidner Jr., and G. J. Miller, *Phys. Rev. B* **64**, 235103 (2001).

⁶C. Magen, L. Morellon, P. A. Algarabel, C. Marquina, and M. R. Ibarra, *J. Phys. Condens. Matter* **15**, 2389 (2003).

- ⁷S. Velez, J. M. Hernandez, A. Fernandez, F. Macià, C. Magen, P. A. Algarabel, J. Tejada, and E. M. Chudnovsky, *Phys. Rev. B* **81**, 064437 (2010).
- ⁸S. B. Roy, M. K. Chattopadhyay, P. Chaddah, J. D. Moore, G. K. Perkins, L. F. Cohen, K. A. Gschneidner Jr., and V. K. Pecharsky, *Phys. Rev. B* **74**, 012403 (2006).
- ⁹F. Casanova, S. de Brion, A. Labarta, and X. Batlle, *J. Phys. D.* **38**, 3343 (2005).
- ¹⁰E. M. Levin, K. A. Gschneidner Jr., and V. K. Pecharsky, *Phys. Rev. B* **65**, 214427 (2002).
- ¹¹Z. W. Ouyang, V. K. Pecharsky, K. A. Gschneidner Jr., D. L. Schlager, and T. A. Lograsso, *Phys. Rev. B* **74**, 024401 (2006).
- ¹²E. M. Levin, *Phys. Rev. B* **80**, 144401 (2009).
- ¹³C. Magen, Z. Arnold, L. Morellon, Y. Skorokhod, P. A. Algarabel, M. R. Ibarra, and J. Kamarad, *Phys. Rev. Lett.* **91**, 207202 (2003).
- ¹⁴Z. W. Ouyang, V. K. Pecharsky, K. A. Gschneidner Jr., D. L. Schlager, and T. A. Lograsso, *Phys. Rev. B* **74**, 094404 (2006).
- ¹⁵E. M. Levin, K. A. Gschneidner Jr., T. A. Lograsso, D. L. Schlager, and V. K. Pecharsky, *Phys. Rev. B* **69**, 144428 (2004).
- ¹⁶L. Tan, A. Kreyssig, J. W. Kim, A. I. Goldman, R. J. McQueeney, D. Wermeille, B. Sieve, T. A. Lograsso, D. L. Schlager, S. L. Budko, *et al.* *Phys. Rev. B* **71**, 214408 (2005).
- ¹⁷J. Szade and G. Skorek, *J. Magn. Magn. Mater.* **196-197**, 699 (1999).
- ¹⁸G. K. Perkins, J. D. Moore, M. K. Chattopadhyay, S. B. Roy, P. Chaddah, V. K. Pecharsky, K. A. Gschneidner Jr., and L. F. Cohen, *J. Phys. Condens. Matter* **19**, 176213 (2007).
- ¹⁹F. Casanova, X. Batlle, A. Labarta, J. Marcos, L. Mañosa, and A. Planes, *Phys. Rev. B* **66**, 100401(R) (2002).
- ²⁰F. Casanova, X. Batlle, A. Labarta, J. Marcos, L. Mañosa, and A. Planes, *Phys. Rev. B* **66**, 212402 (2002).
- ²¹F.-J. Pérez-Reche, F. Casanova, E. Vives, L. Mañosa, A. Planes, J. Marcos, X. Batlle, and A. Labarta, *Phys. Rev. B* **73**, 014110 (2006).
- ²²F. Casanova, A. Labarta, X. Batlle, E. Vives, J. Marcos, L. Mañosa, and A. Planes, *Eur. Phys. J. B* **40**, 427 (2004).
- ²³F. Casanova, A. Labarta, X. Batlle, F. J. Pérez-Reche, E. Vives, L. Mañosa, and A. Planes, *Appl. Phys. Lett.* **86**, 262504 (2005).
- ²⁴V. K. Pecharsky and K. A. Gschneidner Jr., *J. Alloys Compounds.* **260**, 98 (1997).
- ²⁵L. Morellon, J. Blasco, P. A. Algarabel, and M. R. Ibarra, *Phys. Rev. B* **62**, 1022 (2000).
- ²⁶R. B. Griffiths, *Phys. Rev. Lett.* **23**, 17 (1969).
- ²⁷J. L. Dormann, D. Fiorani, and E. Tronc, *Adv. Chem. Phys.* **98**, 283 (1997), p. 326 and references therein.
- ²⁸J. Herrero-Albillos, L. M. Garcia, and F. Bartolomé, *J. Phys. Condens. Matter* **21**, 216004 (2009).
- ²⁹W. Jiang, X. Z. Zhou, G. Williams, Y. Mukovskii, and K. Glazyrin, *Phys. Rev. B* **76**, 092404 (2007).
- ³⁰C. Magen, P. A. Algarabel, L. Morellon, J. P. Araujo, C. Ritter, M. R. Ibarra, A. M. Pereira, and J. B. Sousa, *Phys. Rev. Lett.* **96**, 167201 (2006).
- ³¹A. H. Castro Neto, G. Castilla, and B. A. Jones, *Phys. Rev. Lett.* **81**, 3531 (1998).
- ³²Y. Mudryk, D. Paudyal, V. K. Pecharsky, K. A. Gschneidner, S. Misra, and G. J. Miller, *Phys. Rev. Lett.* **105**, 066401 (2010).
- ³³Z. W. Ouyang, *J. Appl. Phys.* **108**, 033907 (2010).